Violation of time-reversal symmetry in $YBa_2Cu_3O_{7-x}$ films

H.-J. Weber, A. Burau, and J. Blechschmidt
Universität Dortmund, Institut für Physik, D-44221 Dortmund, Federal Republic of Germany
and Hochfeldmagnetanlage der Technischen Universität Braunschweig, Braunschweig, Germany
(Received 7 September 1993)

We present a concept for the search for optical effects which indicates a violation of time-reversal symmetry in high-T_c superconductors. The idea is to investigate the reaction of the material on a magnetic field in a magneto-optical transmission experiment. Below 150 K an annealing field of 400 Oe induces an optical quantity which remains after the field is switched off and which depends on the sign of the field. This signature of broken time-reversal symmetry is confirmed in fields up to 50 kOe. Our results are consistent with a phenomenological theory which takes into account the presence of strains in films. The strains enable a switching of antiferromagnetic domains by magnetoelastic interactions. This interpretation is supported by the dependence of the optical response on $|H|$.

I. INTRODUCTION

Current interest in effects which are a signature of a violated time-reversal (T) symmetry in high-T_c superconductors arises from stimulating theoretical ideas, in particular from the anyon model.[1] Wen and Zee[2] pointed out that spontaneous Faraday effects are a signature of broken T symmetry. However, the first experiments yielded positive[3,4] as well as negative[5] results. On theoretical arguments it was suggested that in the case of two copper oxide planes in a unit cell of high-T_c materials the order of the gauge field will be of "antiferromagnetic" type.[6] In this case no simple spontaneous Faraday effects can be expected. Dzyaloshinskii[7] argued that the symmetry of $YBa_2Cu_3O_{7-x}$ with anyon layers is equivalent to the symmetry of a spin antiferromagnet and indicated a magnetoelectric effect at optical frequencies. Attempts to explain conflicting results by this effect[7,8] finally failed.[9] In addition, Spielman *et al.* obtained with an optical gyroscope null results in transmission[5,10] and reflection.[11] The magnetoelectric effect is observable only in reflection.[7] Thus, the results of Spielman *et al.* show that in their experiments no magnetoelectric effect appears. Recently Lyons *et al.*[12] reported positive and negative results depending on the sample. A check of the same sample in the apparatus of Spielman *et al.* confirmed the existing discrepancies. Lawrence, Szöke, and Laughlin[13] reproduced the experimental techniques of Lyons *et al.* and observed no sign for broken T symmetry.

The seemingly contradictory results in the search for spontaneous effects suggest that either in measurements with positive result an uncontrolled influence of reciprocal optical effects is present or in measurements with negative result the observability of nonreciprocal optical effects is quenched. Tests of the apparatus are always reported, most extensively by Lawrence, Szöke, and Laughlin.[13] Tests on quenching have never been mentioned. This partially discredits the arguments for null results. The results reported by Lyons *et al.*[12] indicate that the origin of discrepancies is not simply a problem of the experimental setups.

The impression of a complex behavior of $YBa_2Cu_3O_{7-x}$ arises also from investigations in our laboratory. Evidence for broken T symmetry was concluded from the influence of a static magnetic field on optical quantities which could be reciprocal and/or nonreciprocal.[4] Measuring the ellipticity induced by a small static field in a film, one of us[14] observed an anomalously strong response in the temperature range from 100 to 150 K with a peak near 110 K. However, in a systematic study of magnetic circular dichroism (MCD), Kerr rotation, and Kerr ellipticity with alternating magnetic fields, we observed no remarkable dependence on temperature.[15]

In nearly all situations where a new phase nucleates (phase transition, crystal growth) the size of domains depends on the duration for passing the transition temperature and on experimental details such as temperature gradients, external forces, etc. In the search for spontaneous nonreciprocal effects, researchers do not know the temperature where broken T symmetry may occur, and also the behavior of anyons in a real experiment is not well known. From remarks about the stability of their reflection apparatus one has to conclude that Spielman *et al.*[11] cool the sample to low temperatures in about half an hour. This cannot be considered to be the best procedure to avoid quenching. Thus, the reported negative results do not necessarily disprove the existence of spontaneous nonreciprocal optical responses in high-T_c materials. On the other hand, the appearance of spontaneous effects is always difficult to control, not only in the present case. Therefore, an experimental procedure with a higher potential for reproducibility and controlled handling is needed. For two reasons a promising alternative is the search for optical quantities induced linearly by an external magnetic field. First, they can be an intrinsic signature of antiferromagnetic ordering. Secondly, in the presence of defects which break the local symmetry the external field can switch antiferromagnetic domains.

Our concept is outlined in Sec. II. We consider the optical properties which are allowed by the symmetry of

0163-1829/94/49(10)/6991(13)/$06.00

$YBa_2Cu_3O_{7-x}$ with an antiferromagnetically ordered anyon structure. Taking into account the strains which are present in a film, magnetoelastic interactions also become allowed. The connection of the field with elasticity points the way to discriminate between magneto-optical responses originating in a broken T symmetry and MCD, which exists independently of any magnetic ordering. As is known from measurements of internal friction,[16] $YBa_2Cu_3O_{7-x}$ shows anelastic relaxation peaks at several distinct temperatures. If a magnetic field is able to couple to anelastic processes, relaxation mechanisms can be visible in magneto-optical measurements, too. In the case of long relaxation times, different results can be expected for static and alternating fields. These considerations and previous observations of anomalous responses in static fields[4,14] motivated us to study systematically optical properties under several experimental conditions. From the considerations in Sec. II we conclude that optimal conditions for detecting a signature of broken T symmetry are obtained by slow cooling in a static magnetic field. With the experimental setup described in Sec. III, a stability of 1 μrad over a period of 12 to 15 h is achieved. The applied fields are small (<400 Oe). For an experiment in high fields (up to 50 kOe) a slightly modified apparatus is used. The importance of demonstrating the correct working of the apparatus has already been mentioned above. Therefore, we include a discussion of misleading effects and the results of test measurements in Sec. III. In Sec. IV the violation of T symmetry is demonstrated by two independent effects. Some further results support our phenomenological theory. In the light of present investigations we briefly discuss in Sec. V reasons for seemingly contradictory results.

II. GENERAL CONSIDERATIONS

A. Optical c tensors

The characteristic feature of a material with broken T symmetry is the appearance of c tensors which describe the magnetic properties.[17] In the case of optical properties the fundamental quantity is the dielectric tensor $\mathcal{E}_{ij}$. Its antisymmetric part can be reduced to the axial gyration vector $\mathcal{G}$:

$$\mathcal{E}_{ij}=\varepsilon_{ij}+ie_{ijk}\mathcal{G}_k \ , \tag{1}$$

where e_{ijk} is the Levi-Cività pseudotensor. Whereas the symmetric part ε_{ij} is an i tensor, $\mathcal{G}_i$ can represent a c as well as an i vector. To distinguish between both contributions we relate the part which is invariant under T operation to the wave vector $\mathbf{k}$:

$$\mathcal{G}_i=G_i^c+g_{ij}^i k_j \ . \tag{2}$$

Here g_{ij}^i is a signature of a structural chirality. G_i^c and $g_{ij}^i k_j$ result in nonreciprocal and reciprocal circular optical effects, respectively. G_i^c exists only in materials exhibiting a magnetization $\mathbf{M}$. To obtain a signature of broken T symmetry in antiferromagnetic crystals with $\mathbf{M}=0$, Eqs. (1) and (2) have to be extended. This can be done by considering the effects of external forces on ε_{ij} and $\mathcal{G}_i$. Here we take into account a magnetic field $\mathbf{H}$ and elastic strains S_{ij}. In the following we will use the notation with contracted indices for ε_{ij} and S_{ij} ($\varepsilon_{ij}=\varepsilon_k$ and $S_{ij}=S_k$ with $k=1-6$). Due to Onsager's principle[18] the product of a c tensor and an i (c) tensor is a c (i) tensor. With this rule and a similar one which holds for the product of polar and axial tensors we obtain the following relations up to second order in H_i and S_i:

$$\underline{G}_i^c=\underline{G}_i^{0,c}+(f_{ij}\underline{H}_j^c)+\underline{\alpha}_{ij}^c S_j+(f'_{ijk}\underline{H}_j^c S_k) +\underline{\alpha}'^c_{ijk}\underline{H}_j^c\underline{H}_k^c+\underline{\alpha}''^c_{ijk}S_jS_k \ , \tag{3a}$$

$$\varepsilon_i=(\varepsilon_i^0)+\underline{\beta}_{ij}^c\underline{H}_j^c+(p_{ij}S_j)+\underline{\beta}'^c_{ijk}\underline{H}_j^c S_k +(p'_{ijk}\underline{H}_j^c\underline{H}_k^c)+(p''_{ijk}S_jS_k) \ , \tag{3b}$$

$$\underline{g}_{ij}=\underline{g}_{ij}^0+(\gamma_{ijk}^c\underline{H}_k^c)+\underline{w}_{ijk}S_k+(\gamma'^c_{ijkl}\underline{H}_k^c S_l) +\underline{w}'_{ijk}\underline{H}_k^c\underline{H}_l^c+\underline{w}''_{ijkl}S_kS_l \ . \tag{3c}$$

Here all quantities without the superscript c denote i tensors; axial tensors are indicated by letters with underbars. In the following, notations are used without the explicit distinction between different kinds of tensors. For studying the restrictions imposed by symmetry on the existence of physical properties we follow the proposal by Dzyaloshinskii.[7] He suggested that in the presence of anyons the symmetry is equivalent to that of a two-dimensional spin system in the copper oxide planes. In this sense of equivalence our usage of quantities like "magnetization" or "antiferromagnetic order" should be understood. For the expected antiferromagnetic order, the magnetic point-symmetry group (MPSG) of $YBa_2Cu_3O_{7-x}$ is $m'm'm'$.[7] Applying these space-time operators to Eq. (3), only the terms in parentheses survive. Some additional restrictions are imposed on the existence of distinct tensor components. In Eq. (3) all optical quantities and coefficients of the material are complex. The indices are referred to a coordinate system with axes x_1,x_2,x_3 parallel to the crystallographic axes a,b,c of $YBa_2Cu_3O_{7-x}$.

Equation (3) shows that the only optical quantity which can give a signature of broken T symmetry is g_{ij} induced by a magnetic field and/or by a coupling of field and strain. As g_{ij} results in a reciprocal circular optical effect it can be observed in transmission only. Thus, for an optical experiment the sample has to be a film. For practical reasons the magnetic field and the light beam are chosen parallel to the film normal. In a c-axis-grown film this is the only well-defined crystallographic orientation. Due to the random orientation of a and b axes, linear anisotropies are averaged out on a macroscopic scale. Considering only contributions which can be observed with the experimental setups described in the next section, Eq. (3) reads for MPSG $m'm'm'$ explicitly

$$G_3=f_{33}H_3+f'_{33i}H_3S_i \tag{4a}$$

$$\varepsilon_6=\varepsilon_6^0+p_{66}S_6+p''_{654}S_5S_4+p''_{66i}S_6S_i \tag{4b}$$

$$g_{33}=\gamma'_{3336}H_3S_6 \tag{4c}$$

for $i=1,2,3$.

From Eq. (4) at once two problems arise. The first is

the discrimination between a field-induced g_{33} (Eq. 4c) and the usual Faraday effect (Eq. 4a). The second is the occurrence of antiferromagnetic domains. Due to a reversal of all internal magnetic moments, the c tensors in Eq. (3) can be positive or negative. To handle both problems we take into account the presence of defects in films and the rather uncommon elastic properties of $YBa_2Cu_3O_{7-x}$. In the following sections the ideas for obtaining optimal experimental conditions to detect broken T symmetry are evaluated.

B. Influence of defects

Figure 1 shows two idealized standard situations for $YBa_2Cu_3O_{7-x}$ grains grown on a MgO substrate with orientation {100}. In Fig. 1(a) it is assumed that due to the epitaxial growth at the substrate-film interface the lattice constants a and b of the grain are equal to the lattice constant a_{MgO} of the substrate. As a_{MgO} is about 10% larger than $\bar{g}=(a+b)/2$, the order of magnitude for the strains in films can be 0.1. Towards the free face of the film a linear decrease of the deformation is assumed. As a consequence the mirror plane perpendicular to the c axis is destroyed. Figure 1(b) shows a similar grain as Fig. 1(a) but as a crystallographic twin. In practice twinning appears in all grains. The twin boundary is used as the reference line which exhibits a minimum of deformation. In this grain all mirror planes are destroyed, leaving an opposite sign of chirality in the two twins.

As the grains are small and their number is large in a film, the reduction of symmetry cannot be neglected. Its influence on optical properties can be taken into account by associating the grains in Fig. 1(a) and 1(b) with the effective MPSG's $m'm'2$ and 2. Another approach is to leave the MPSG $m'm'm'$ unchanged and to consider the effect of the strains and the gradient of strains which are visible in Fig. 1. From the point of view of symmetry both approaches are equivalent but the latter seems to be more conclusive.

The defect model in Fig. 1(a) is characterized mainly by the strains S_1,S_2,S_4,S_5 and the gradients $\partial S_1/\partial x_3,\partial S_2/\partial x_3$. The most important consequence is

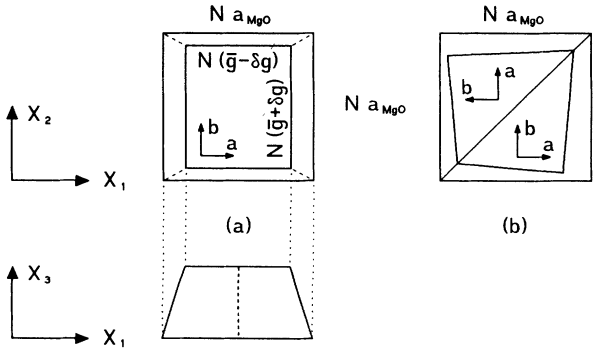

FIG. 1. Simple models of $YBa_2Cu_3O_{7-x}$ grains grown on MgO. a_{MgO} is the lattice constant of MgO. $\bar{g}$ is the average of a and b lattice constants of $YBa_2Cu_3O_{7-x}$, δ_g half its difference, and N the number of unit cells involved.

the appearance of new effects which are a characteristic sign for broken T symmetry:

$$G_3=\alpha^*_{3i3}(\partial S_i/\partial x_3)\ , \tag{5a}$$

$$T_j=\delta^*_{ij33}(\partial S_i/\partial x_3)H_3\ , \tag{6a}$$

for $i=1,2;j=1,2,3$.

Here T_j denotes stresses and α^*_{3i3}, δ^*_{ij33} are c tensors. The additional features in Fig. 1(b) are a strain S_6 and a twisting about x_3. We describe the latter by the axial tensor component $\Omega_{33}=\partial\omega_3/\partial x_3$, where ω_3 is the rotation of unit cells about x. The new effects described by c tensors are

$$\varepsilon_6=\beta^*_{6333}\Omega_{33}H_3\ , \tag{5b}$$

$$T_6=\pi^*_{6333}\Omega_{33}H_3\ . \tag{6b}$$

Due to the magnetoelastic interactions given in Eq. (6), H_3 induces a stress T_i (T_6) which meets the spontaneous strain S_i^0 (S_6^0). The product $T_iS_i^0$ ($T_6S_6^0$) reduces the deformation energy only for one sign of δ^*_{ij33} (π^*_{6333}). Thus, all antiferromagnetic domains with the wrong sign will tend to be switched. This correlates the sign of $\delta^*_{ij33}\partial S_i/\partial x_3$ and $\alpha^*_{3i3}\partial S_i/\partial x_3$ ($\pi^*_{6333}\Omega_{33}$ and $\beta^*_{6333}\Omega_{33}$) for all domains to the sign of the external field and homogenizes the optical response of the sample. This is our basic idea for making the presence of an antiferromagnetic structure visible.

The defect models presented in Fig. 1 are not the only origin for the loss of the center of symmetry which results in the additional effects given in Eqs. (5) and (6). A defect which does the same is the spiral growth of grains.[19] Furthermore, there is experimental evidence that the absence of a center of symmetry can be an intrinsic property of the structure, at least at low temperatures.[20] The existence of monoclinic strains (S_4,S_5,S_6) in films has already been shown by x-ray diffraction.[21]

C. Connection between magneto-optical effects and elastic properties

$YBa_2Cu_3O_{7-x}$ exhibits some unusual elastic properties. Here we point out its strong nonlinear elasticity[22] and the presence of slow anelastic-relaxation processes at low temperatures.[16] Nonlinear elasticity is defined by the coefficient c^* in the stress-strain relation

$$T=cS+c^*S^2\ , \tag{7}$$

where the tensor character has been neglected. From the dependence of the velocity of ultrasonic waves on hydrostatic pressure, a magnitude of $c^*/c\approx-300$ has been concluded.[22] The magnitude of strains at the interface can be up to $S\approx0.1$ (see Sec. II B). Inserting these values into Eq. (7) shows the importance of nonlinear contributions in films.

Below about 250 K elastic constants show a hysteresis for cycles of cooling and warming[23] and at constant temperatures the elastic response drifts on a time scale of minutes.[24] Connected to these phenomena are slow relaxation processes. Above T_c measurements of internal friction in ceramics peak mainly near 220 and 115 K.[16]

In single crystals the peak at 115 K is slightly shifted towards higher temperatures.[25] The peak near 220 K is observed also in Cu_2O.[26] Its origin seems to be a structural phase transition as shown by a jump in the elastic constants.[27] There is no commonly accepted interpretation for the peak near 115 K.

In a film stresses are generated mainly on the substrate-film interface. Their impact on the grains is the deformation shown in Fig. 1. Roughly speaking, the effect of both phenomena, nonlinear elasticity and anelastic relaxation, is the same. They increase strains compared to a simple linear elastic response, which in turn enhances all optical effects where strains are involved. Strains appear in Eqs. (4) and (5). Only in the presence of an antiferromagnetic structure can stresses be induced linearly by an external field (Eq. 6). If these stresses are transformed into strains by slow relaxation processes, the linear magneto-optical effect is enhanced and can be different for static and alternating fields. This is our idea for discriminating between magneto-optical responses based on a magnetic structure and the usual Faraday effects.

As a first step it is necessary to verify that in alternating fields only Faraday effects are observed. With a magnetic field alternating at a frequency of 800 Hz and with an amplitude smaller than 400 Oe we have determined magnetic circular dichroism in transmission and Kerr ellipticity and Kerr rotation in reflection. A full description of these experiments is given elsewhere.[15] The three independent measurements enabled a consistency check which verified that the real part $\partial G_3'/\partial H_3$ and the imaginary part $\partial G_3''/\partial H_3$ of the Faraday effect were observed. Neither in transmission nor in reflection was any anomalous dependence on temperature detected. Magnetic circular dichroism exhibited a slight linear increase with temperature, which is in accordance with results reported by Krichevtsov *et al.*[28] Furthermore, we found that the magnitude of MCD determined on films which were prepared in three different laboratories was the same. From these investigations we are sure that in sample A (see Sec. III A) at 150 K the MCD is

$$\partial\sigma_{\mathrm{NR}}/\partial H_3 = 2\pm 0.2\times 10^{-9}\ \mathrm{rad/Oe}\ . \tag{8}$$

D. Consequences for experiments

We have tried a rough estimation for a field- and strain-induced reciprocal circular dichroism (Eq. 4c) by considering the magnitude of similar effects shown by other crystals. Strains are present in the film (Sec. II B), and strain-induced optical activity was reported for $NaClO_3$.[29] Magnetic-field-induced linear birefringence was observed in the antiferromagnet CoF_2 (Ref. 30) and circular and linear birefringence differ typically by a factor a/λ, where a is an intermolecular distance. With these ingredients we obtain for a film of 300-nm thickness a reciprocal circular dichroism of 10^{-9}–10^{-8} in a field of 1 kOe. This order of magnitude is terribly small. It indicates that a signature of broken T symmetry can be expected only if two favorable conditions are met simultaneously. These are a potentially large effect of the antiferromagnetic system and extraordinarily large strains.

In our present experiments samples are annealed in a magnetic field to utilize slow relaxation processes. This needs a high stability of the apparatus. Furthermore, our experimental setups are able to detect all optical properties given in Eqs. (4b) and (5) but suppress substrate effects. As shown by Eq. (3) a proof for the existence of c tensors is a reciprocal optical quantity induced linearly by a magnetic field. However, in a transmission experiment on a film it is difficult to identify the reciprocal character of an optical quantity. Furthermore, our phenomenological theory does not allow us to predict what will be the leading effect. Therefore, it is not useful to neglect quantities which might appear. Nevertheless, we need clear experimental signatures to identify broken T symmetry.

The basic optical quantities we are concerned with are circular birefringence ρ, circular dichroism σ, linear birefringence g, and linear dichroism p. Furthermore, we have to take monoclinic deformations into account. As a consequence the principal axes for g and p differ from the crystallographic a,b axes by the angles ζ and ξ, respectively. In the approximation that each optical anisotropy can be described in the absence of the others we obtain the following connection to the tensor components in Eqs. (4) and (5):

$$\rho_{\mathrm{NR}} = (\pi L/\bar{n}'\lambda)G_3'\ , \tag{9a}$$

$$\sigma_{\mathrm{NR}} = (\pi L/\bar{n}''\lambda)G_3''\ , \tag{9b}$$

$$g\tan 2\zeta = (\pi L/\bar{n}'\lambda)\varepsilon_6'\ , \tag{10a}$$

$$p\tan 2\xi = (\pi L/\bar{n}''\lambda)\varepsilon_6''\ . \tag{10b}$$

Here single- and double-primed quantities correspond to the real and the imaginary parts of n, G_3, and ε_6. L is the thickness of the sample and $\bar{n}$ is an average refractive index. Reciprocal ρ_R and σ_R are obtained by a replacement of G_3 with $g_{33}k_3$. In a real medium single- and double-primed quantities are mixed. This, however, does not change the principal relations.

As we use a rather large laser spot in our experiments and with reference to remarks above about the magnitude of the properties, it is reasonable to assume that if an effect is observed the field has already switched the antiferromagnetic domains. In the presence of spontaneous strains, Eqs. (5a) and (9) show that a spontaneous σ_{NR} survives after the field is switched off. The sign of this spontaneous effect has to depend on the sign of the field applied before. In Eqs. (4c) and (5b) the sign of the c tensors depends on the sign of H and the optical response on the magnitude of H. This results in a dependence of σ_R and $p\tan 2\xi$ or $g\tan 2\zeta$ on $|H|$, which is another signature of broken T symmetry. Additional evidence arises from a possible enhancement by anelastic-relaxation processes, which should result in a specific dependence on temperature and in a magnitude of optical responses to H which is larger than the value given in Eq. (8).

III. EXPERIMENTAL TECHNIQUE

A. Samples

Measurements were carried out on two c-axis-oriented $YBa_2Cu_3O_{7-x}$ films. For both samples the substrate is MgO of thickness 1 mm. Sample A was used for measurements in low fields only. The thickness of the film is 300 nm and its T_c is 85 K. The substrate is wedge shaped (wedge angle 4°) which avoids interferences in the substrate but introduces a small linear dichroism of 0.1 mrad.

Due to simple geometric reasons it was not possible to use a wedge-shaped sample for the measurements in high fields. Therefore, the substrate of sample B is plane parallel. The film shows a T_c of 90 K and the thickness is 220 nm. In addition to the measurements in high fields, sample B has also been used in one low-field experiment in order to check the main results obtained with sample A.

As we are searching for a signature of an antiferromagnetic state, it is important to verify that the samples are not contaminated by the tetragonal phase ($x > 0.5$) which is known to be antiferromagnetic. A separation into a metallic and an insulating phase can happen due to some content of hydrogen, which in principle can be adsorbed by the samples from air. Although it is rather unlikely that a small amount of hydrogen is able to create an ordered antiferromagnetic state on a macroscopic level, we have checked this by absorption measurements between 1 and 6 eV. A characteristic feature of the tetragonal phase is a strong absorption peak near the photon energy of 4 eV.[31] In addition we have measured absorption in the near-infrared region (2700–3200 nm) where the typical OH bands appear. From both kinds of measurements we obtained no hint of the presence of the tetragonal phase. Furthermore, the magnetic susceptibility of the tetragonal phase exhibits a strong $1/T$ dependence.[32] This should be visible in the temperature dependence of the MCD, too. Indeed it is observed in samples prepared in a wet atmosphere.[33] Our samples do not show any increase of MCD towards low temperatures.[15]

B. Experimental setups

1. *Apparatus A*

The experimental setup used for low-field measurements is shown in Fig. 2(a). In order to achieve a high stability as few optical elements as possible were used. The lens focuses the light beam only slightly. The diameter of the beam at the position of the sample is about 90 μm. The coil which produces the magnetic field is incorporated in the cryostat and it is cooled together with the sample. For fields smaller than 400 Oe the cooling power of the cryostat is sufficient to avoid a noticeable warming by the currents. The electro-optical modulator is driven at the frequency $\nu = 1.3$ kHz. At the same frequency the change of intensity $I(\nu)$ detected by the photodiode is recorded by lockin techniques. The total intensity is measured simultaneously.

The modulator is a thin (thickness 1.5 mm) plane-

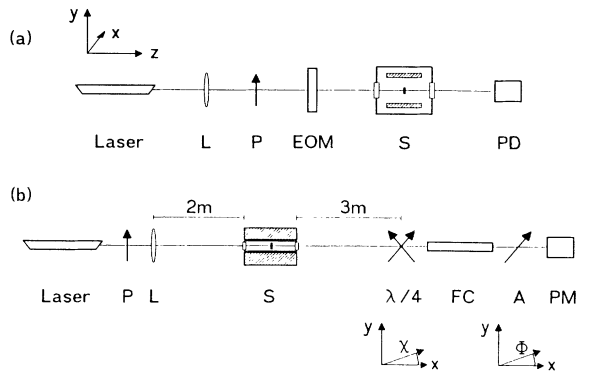

FIG. 2. Schematic setups for (a) low- and (b) high-field experiments. L: lens, P: polarizer, EOM: electro-optical modulator, S: sample, PD: photodiode, $\lambda/4$: quarter-wave plate, FC: Faraday cell, A: analyzer, PM: photomultiplier; χ and Φ denote the orientation of the quarter-wave plate and the analyzer, respectively.

parallel (001) plate made from a large KH_2PO_4 (KDP) single crystal. The light wave is traveling along the optical axis and a longitudinal electric field induces a birefringence $g_m = g_{m0}\cos(2\pi\nu t)$ that is parallel to the crystallographic [110] direction of KDP. Its [100] axis is parallel to the x axis of the laboratory system shown in Fig. 2. The electro-optical effect results in a modulated ellipticity of the originally linearly polarized wave. The modulation amplitude is 35 mrad which is determined by introducing a quarter-wave plate and an analyzer between the modulator and the detector. A larger modulation amplitude requires a higher field, which reduces the stability of the modulator.

Our calculation of the optical transfer matrix of the film is based on Jones calculus with definitions reported previously.[34] As the linear birefringence g and linear dichroism p of each grain are large, terms up to L^2 (L being the thickness of the film) for linear anisotropies have been considered, whereas for ρ and σ only terms linear in L are kept. Assuming an ideal modulator we obtain for the normalized intensity $I(\nu)$ which oscillates at the frequency of the modulator:

$$I(\nu) = -[\sigma + pg\sin(2\zeta - 2\xi)]4g_m(\nu) . \tag{11}$$

The second term is a consequence of monoclinic deformations. For small angles ζ, ξ it is approximately proportional to

$$(\pi L/\lambda)\left[\frac{p}{\bar{n}'}\varepsilon_6' - \frac{g}{\bar{n}''}\varepsilon_6''\right] .$$

Both terms in Eq. (11) can appear only for an absorbing material. Thus, the influence of the substrate is strongly suppressed. Equation (11) contains neither g nor p as separate terms. Therefore, all linear anisotropies which can be introduced by imperfect optical elements (substrate, cryostat windows, lenses, polarizers) and which are subjected to the conditions of the environment (temperature drifts, mechanical vibrations) contribute to the signal only in second order. As a consequence, the influence of changes of the parasitic effects is strongly

suppressed. This guarantees that $I(\nu)$ can be detected with high stability.

In practice the modulator is not ideal. As it is thin a quite exact preadjustment of its optical axis parallel to the wave vector is possible. The residual misfit results in a small birefringence g_s with the orientation ζ_s. The transfer matrix which is obtained by superposing g_s with the electric-field-induced birefringence g_m is given in Ref. 34. The interaction between g_s and the linear dichroism p of the film can be neglected because of the random orientation of grains. However, there exists a linear dichroism p_w of the wedge oriented at the angle $\xi_w=0$. In addition, under the action of a magnetic field the substrate exhibits a Faraday rotation ρ_{MgO} which is much larger than all effects of the film, and its influence on $I(\nu)$ has to be considered in detail. Taking these parameters into account we obtain in addition to Eq. (11) the parasitic signal

$$I(\nu)_p=-[p_w g_s \sin 2\zeta_s + p_w g_s \rho_{\mathrm{MgO}} \sin 2\zeta_s]8g_m(\nu) . \tag{12}$$

The different contributions to the signal detected by apparatus A of Fig. 2(a) may be abbreviated as

$$\sigma_{\mathrm{eff}}=\sigma_{\mathrm{NR}}+\sigma_R+\sigma_M+\sigma_p=-I(\nu)/4g_{m0} , \tag{13}$$

where g_{m0} is the modulation amplitude. In Eq. (13), σ_{NR} (σ_R) denote the nonreciprocal (reciprocal) circular dichroism, σ_M represents the monoclinic term of Eq. (11), and σ_p is the sum of the parasitic effects given in Eq. (12).

2. *Apparatus B*

The experimental setup used for measurements in high fields is shown in Fig. 2(b). The incoming light wave is polarized along the x axis of the laboratory system. The cryostat is in the center of a Bitter magnet. The rotation Θ and the ellipticity ϵ induced by the sample and by the cryostat windows are assumed to be small. A principal axis of the quarter-wave plate is nearly parallel to the x axis. The Faraday cell is driven at the frequency $\nu=130$ Hz with an amplitude of rotation of 1.5 mrad. When the azimuthal position Φ of the analyzer satisfies the condition $I(\nu)=0$ then

$$\Phi_0=(-\epsilon+\chi-\Theta\Delta)/(1-\Delta-2\Theta^2) ,$$

where Δ is the error parameter of the quarter-wave plate.[34] With the anisotropy parameters in Eqs. (9) and (10), the ellipticity of the film is given by

$$\epsilon_{\mathrm{film}}=\sigma+pg \sin(2\zeta+2\xi+4\alpha)-g \sin(2\zeta+2\alpha) , \tag{14}$$

where α measures the orientation of the a axis of a grain with respect to the direction of light polarization. In a film the last term is averaged out but we cannot neglect other sources of linear birefringence. Collecting all error parameters in the term ϵ_p, including χ and Δ of the quarter-wave plate, the observed ellipticity can be written as

$$\epsilon=\sigma+pg \sin(2\zeta+2\xi+4\alpha)+\epsilon_p=\sigma_{\mathrm{NR}}+\sigma_R+\sigma_{\mathrm{LA}}+\epsilon_p . \tag{15}$$

Again, σ is σ_{NR} or σ_R. Notice that the term $\sigma_{\mathrm{LA}}=pg \sin(2\zeta+2\xi+4\alpha)$, which describes the influence of linear anisotropies, is not identical with the monoclinic term σ_M measured with apparatus A. For small angles ζ,ξ, σ_{LA} is approximately proportional to

$$(\pi L/\lambda)\left\{\left[\frac{p}{\bar{n}'}\varepsilon_6'+\frac{g}{\bar{n}''}\varepsilon_6''\right]\cos 4\alpha+pg \sin 4\alpha\right\} .$$

ϵ_p arises from the interaction of the Faraday rotation Θ_{FR} of the substrate and the cryostat windows with the error parameters of the optical elements. Those of the quarter-wave plate, χ and Δ, have already been mentioned. A second source for misleading effects is the strain birefringence g_0 due to the substrate which may have the arbitrary orientation ζ_0. Finally, there is the conversion of Θ_{FR} into ellipticity by interferences in the substrate and the windows. These contributions to the error parameter ϵ_p contain a spontaneous and a field-dependent part. In the high-field experiments, we are only interested in the effect which depends on H for constant temperatures. Therefore, ϵ_p is rescaled to zero before the field is switched on. The field dependence of ϵ_p can be shown to be

$$\epsilon_p=[\Delta+g_0 \cos 2\zeta_0+2c' \sin(2\delta L')+2c'' \cos(2\delta L')]\Theta_{\mathrm{FR}} + [2\chi+0.5g_0 \sin 2\zeta_0]\Theta_{\mathrm{FR}}^2 , \tag{16}$$

where $c=c'+ic''$ is a complex reflection coefficient and $\delta L'$ is the phase retardation of the wave in a transparent medium of thickness L'. It should be noted that Eq. (16) represents average effects of the substrate and both cryostat windows. $\delta L'$ of the substrate depends on temperature, which causes an oscillation of ϵ_p.

C. Test measurements

1. *Apparatus A*

Equation (12) shows that the linear dichroism p_w of the wedge reacts with the residual linear birefringence g_s of the modulator. In fact, g_s can be considered to be the sum of all birefringences (cryostat windows, substrate, modulator) in the beam. The same holds for p_w. To control these error parameters at one edge of sample A a 1-mm-wide stripe is not covered by the film. By a small shift of the cryostat this part can be measured. Adjusting the modulator σ_p is minimized. In this position a field of 400 Oe, which produces a Faraday rotation of 0.4 mrad, does not affect $I(\nu)$ within the sensitivity of about 0.5 μrad. Thus, the last term in Eq. (12) can be neglected.

Repeating this procedure several times $I(\nu)$ reproduces within a limit of only 8 μrad. The same procedure with a spot near the center of the sample, where it is covered by the film, results in a reproducibility of 1.7 μrad. We attribute the better reproducibility on the film to a more homogeneous strain birefringence of the substrate near its center than at its edges and to a smoother

surface of the sputtered film compared to the polished substrate. From the above results we conclude that the limit for absolute determination of film parameters is 8 μrad but that relative changes can be detected more accurately. This point is tested with a EuS film. EuS exhibits a strong magnetic circular dichroism at the wavelength $\lambda=633$ nm with a paramagnetic dependence on temperature.[35] At room temperature σ_{eff} is adjusted to less than 1 μrad. As shown by the zero-field values in Fig. 3, σ_{eff} does not change with temperature. Thus, the apparatus is stable. The values taken under applied field follow a Curie-Weiss law, demonstrating that the apparatus works correctly.

2. *Apparatus B*

As shown in Eq. (14) the apparatus B for measurements in high fields detects also linear birefringence. As a consequence it is less stable than apparatus A. On the other hand, apparatus B is used for determining the field dependence at a constant temperature and there is a need for stability only for the time the field is applied. A test measurement performed at two different temperatures is shown in Fig. 4. For the period of a field run the apparatus is stable. The average error is about 50 μrad.

In order to identify the misleading influences of the Faraday rotation [Eq. (16)], Θ_{FR} must be determined. For these measurements the apparatus is modified, which can be done in two ways. In the first configuration the quarter-wave plate in Fig. 2(b) is removed. The extinction position of the analyzer $[I(\nu)=0]$ is then given by

$$\Phi_0=[1+2c'\cos(2\delta L')-2c''\sin(2\delta L')]\Theta_{\text{FR}} .$$

which contains the interference term in a similar way as Eq. (16). For the second configuration, at first $\Phi_0=0$ is adjusted and then the Faraday cell and the quarter-wave plate in Fig. 2(b) are interchanged. Rotation of the quarter-wave plate to the position where $I(\nu)=0$ yields

$$\chi_0=(1-2\Delta)\Phi_0 .$$

Figure 5 shows results for both kinds of measurements performed at 91 K. The slopes $\partial\Phi_0/\partial H$ and $\partial\chi_0/\partial H$ are

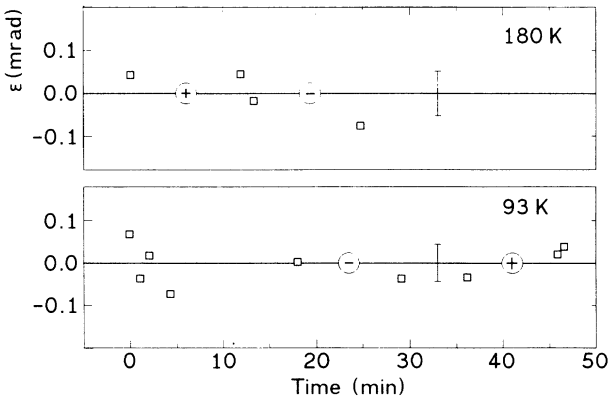

FIG. 4. Test measurements of ϵ using setup B. + and − indicate times where a field of 50 kOe has been applied. The field was turned off before the next data point was taken. The error bars represent the scatter of the data.

slightly different. This difference enables a determination of the error parameter of the quarter-wave plate ($\Delta=0.016\pm0.009$).

$$\partial\Phi_0/\partial H=1.69\pm.01\ \mu\text{rad/Oe}$$

is a measure of Θ_{FR} of the substrate and the windows. In addition, Fig. 5 presents results obtained at room temperature without cryostat windows.

$$\partial\Phi_0/\partial H=0.91\pm0.02\ \mu\text{rad/Oe}$$

is the Faraday rotation of the substrate, which agrees well with data for MgO from literature.[36] The smaller effect of the windows is mainly due to their position at the ends of the magnetic coil where the field is smaller than at the center. The Faraday rotation is determined at several temperatures to obtain the amplitude of interference oscillations, the strain birefringence of the substrate is measured, and the accuracy for the adjustment of the quarter-wave plate is checked. From these data we are able to estimate the systematic error which can be introduced by the Faraday rotation in a measurement of the

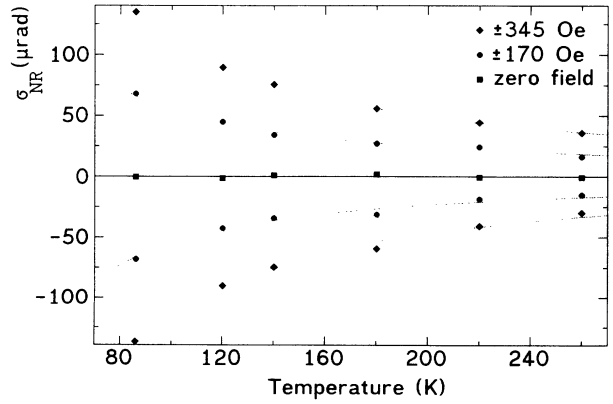

FIG. 3. Test measurements of σ_{NR} on a EuS film using setup A. The lines represent a fit according to $\sigma_{\text{NR}}=\sigma_0+C/(T-18\ \text{K})$.

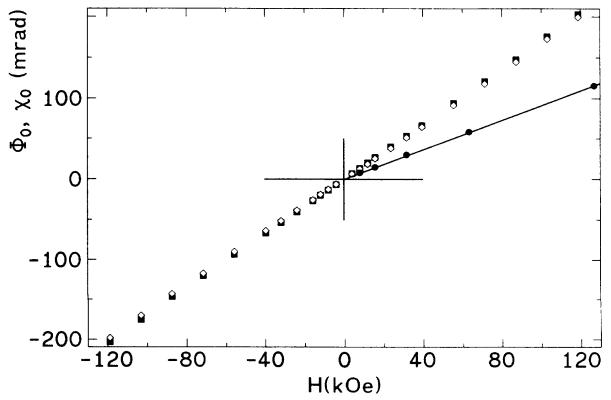

FIG. 5. Test measurements of Φ_0 (■) and χ_0 (◇) at 91 K using setup B. The ● show Φ_0 for room temperature measurements without cryostat windows.

field-induced ellipticity. The result is

$$\delta\epsilon_p = \pm 0.06(\mu\text{rad/Oe})H \pm 0.05\times 10^{-12}(\text{rad/Oe}^2)H^2 \ . \quad (17)$$

Notice that the value of 0.06 μrad/Oe is mainly due to the interference term and, therefore, at most temperatures it will be smaller. Figure 6 presents ϵ of $YBa_2Cu_3O_{7-x}$ on MgO as a function of H for 180 and 93 K. Each symbol represents the average of two values, one taken on increasing and the other on decreasing the field strength. In almost all cases the difference of the two values is smaller than the size of the symbols in Fig. 6. The average error, the linear, and the quadratic response are 10 (22) μrad, -0.001 (0.012) μrad/Oe, and -1.2 $(-2.2)\times 10^{-12}$ rad/Oe^2 for 180 (93) K. For both temperatures the average errors and the linear slopes are compatible with the data given in Fig. 4 and in Eq. (17), respectively. This is not the case for the quadratic terms. Thus, we conclude that $YBa_2Cu_3O_{7-x}$ exhibits an intrinsic nonlinear magneto-optical effect.

IV. RESULTS AND DISCUSSION

If not stated otherwise, all measurements in this section have been performed with the sensitive apparatus A on sample A. We start with experiments which demonstrate the existence of monoclinic strains and of extraordinary optical responses to static fields.

A. Spontaneous effects

In a first run σ_{eff} is adjusted to a value below 1 μrad at a temperature of 260 K. The sample is continuously cooled down to 86 K, just above T_c, and then warmed up to the starting temperature. The rate of temperature changes is 1.5 K/min. The results are shown by curve α in Fig. 7. Notice that at the end of the temperature cycle the starting value is reproduced, which demonstrates the stability of the apparatus. In particular in the range from 160 to 260 K the scattering of values is larger than 1 μrad. We assume that processes associated with elastic anomalies near 220 K are responsible for the scattering. Therefore, in a second run the sample is kept for 20 h at about 180 K before the temperature is changed step by step with an average rate of 0.8 K/min. As shown by curve β in Fig. 7 the scattering of the spontaneous σ^0_{eff} is significantly smaller than in the first run. In the following measurements the procedure of the second run is adopted.

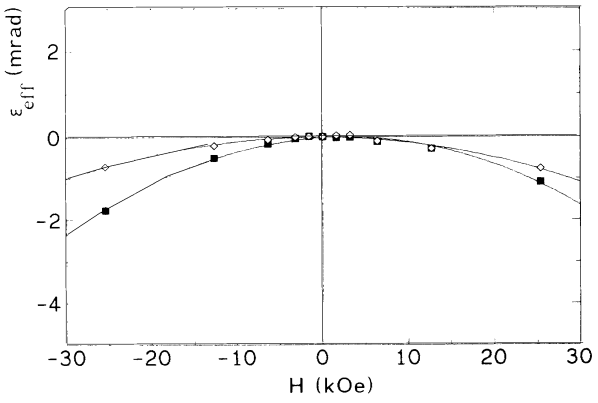

FIG. 6. Test measurements of the ellipticity ϵ_{eff} at 180 K (◇) and 93 K (■) using setup B.

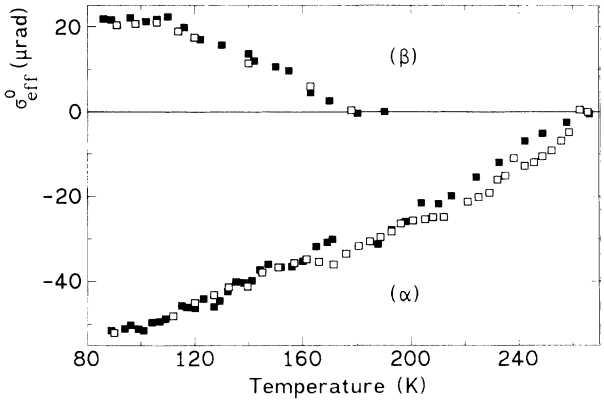

FIG. 7. Spontaneous σ^0_{eff} measured during two temperature cycles. Full symbols are taken during cooling, open symbols during warming. In cycle β the rate of temperature change is a factor of 2 smaller than in cycle α.

It is not unusual that $YBa_2Cu_3O_{7-x}$ films show spontaneous effects in transmission. They have been observed by two groups using circular dichroism spectrometers, too.[37] These spectrometers are sensitive to the same optical quantities as our experimental setup. We attribute the spontaneous σ^0_{eff} to the monoclinic effect σ_M. A possible explanation for an observable σ^0_{eff} is the elastic interaction of the grains with the substrate. As the latter is a single crystal it can homogenize the local stresses at the interface. The magnitude of $\partial \ln\sigma^0_{\text{eff}}/\partial T = 10^{-2}$ K^{-1} shown by both curves in Fig. 7 points to a nonlinear mechanism. In the case of a linear relationship one would expect a value similar to the magnitude of thermal expansion [10^{-5} K^{-1} (Ref. 38)] or of thermoelastic coefficients [10^{-4} K^{-1} (Ref. 16)].

Figure 7 reveals two kinds of monoclinic domains. In curve β $\partial\sigma^0_{\text{eff}}/\partial T < 1$. We attribute this behavior to domains we will call type I. In curve α the signs are opposite, which we will name type-II-domain behavior. To analyze the size of the domains, σ^0_{eff} was determined for eight different spots separated by 190 μm. The starting temperature is 170 K. At this temperature the average value is rescaled to zero. The temperature is decreased step by step and at several temperatures σ^0_{eff} is determined for the eight different spots separately. The results for 170 and 86 K are presented in Fig. 8. Obviously σ^0_{eff} can be rather homogeneous on a scale of 200–300 μm. Due to $\partial\sigma^0_{\text{eff}}/\partial T < 1$, spots 2,3,4,8 belong to domains of type I. Spots 1,5,6,7 represent type-II domains.

Studying the dependence of σ^0_{eff} on temperature in detail we find a different behavior for the two types of domains. Figure 9 (type I) shows a linear dependence above 120 K. Between 110 and 145 K in Fig. 10 (type II) $\sigma^0_{\text{eff}} \sim T^2$ with a maximum at the temperature 155±5 K

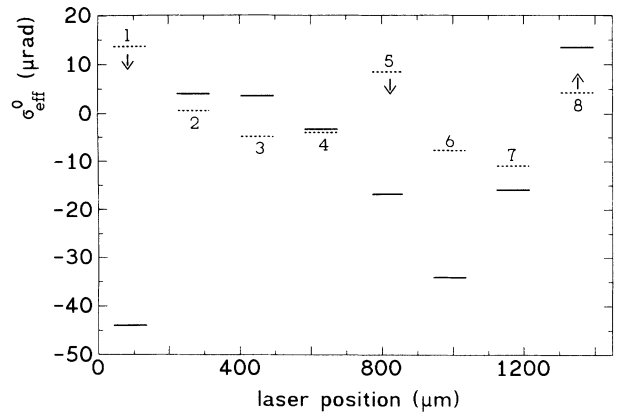

FIG. 8. Values of σ^0_{eff} for eight different spots on the sample at 170 K (dashed lines) and 86 K (solid lines). Arrows indicate decreasing temperature.

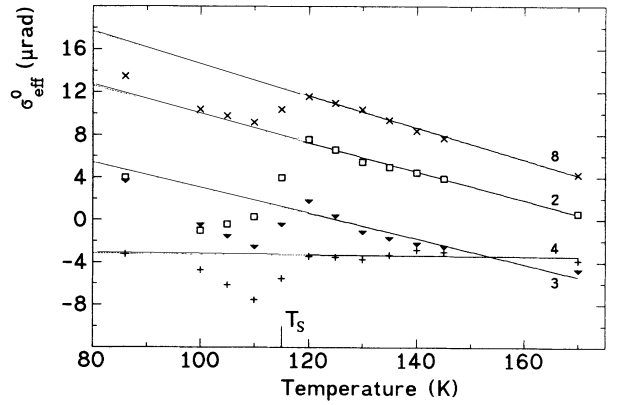

FIG. 9. Temperature dependence of spontaneous σ^0_{eff} of type-I domains. Different symbols indicate different spots on the sample. The numbering of spots is the same as in Fig. 8.

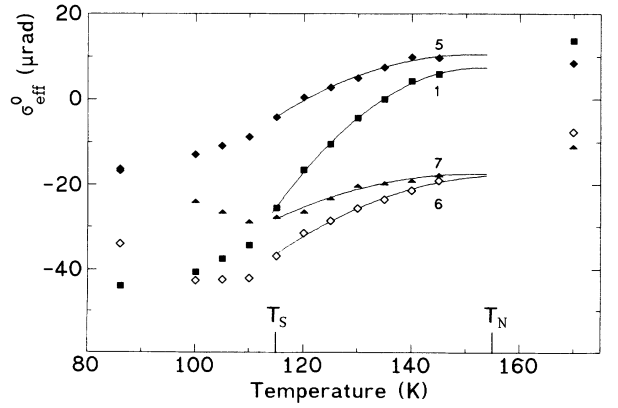

FIG. 10. Temperature dependence of spontaneous σ^0_{eff} of type-II domains. The numbering of spots is the same as in Fig. 8.

which we will name T_N. A common feature in Figs. 9 and 10 is a change of slope near 115 K. We will name this temperature T_S. T_S coincides with the temperature range where the anelastic relaxation is observed.[16] The discontinuity of slopes in Figs. 9 and 10 at T_S indicates that these processes are present in films, too.

B. Extraordinary magneto-optical responses

The first test for an interaction of a magnetic field with anelastic-relaxation processes is performed in the following way. At a fixed temperature σ_{eff} is rescaled to zero in zero field and then H is applied. Results for 180 and 86 K are shown in Fig. 11. There is obviously no remarkable effect. The average slope for both temperatures is $\partial\sigma_{eff}/\partial H = 3\pm2\times10^{-9}$ rad/Oe. This is compatible with the MCD observed with alternating fields[15] and with the apparatus accuracy of 1 μrad. The reproducibility of zero-field values in Fig. 11 demonstrates the absence of thermal drifts when the current is flowing through the magnet coil.

Figure 12 shows that at 120 K, which is in the temperature range where anelastic-relaxation processes are present, the reaction of the material to magnetic fields is completely different than in Fig. 11. The zero-field values at 130 and 120 K before and at 120 K after field treatment demonstrate that it is not possible to trace back the impact of H on σ_{eff} to uncontrolled thermal influences or to drifts of the apparatus. Its dependence on time, its magnitude, and the remanent alteration of the material rule out a simple explanation by MCD. Due to the long relaxation times obviously present in Fig. 12, it is not astonishing that the values taken during field treatment show some stronger scattering than expected from the accuracy of the apparatus. The magnitude of the remanent change in Fig. 12 is ten times larger than the MCD observed with alternating fields and by a factor of 30 larger than the reversible quadratic effect observed in high fields at 180 and 93 K (Fig. 6). Its specific dependence on time and the temperature range for the appearance of this extraordinary magneto-optical response show its connection to anelastic-relaxation processes. Strictly speaking, a remanent alteration of the material is not a characteristic

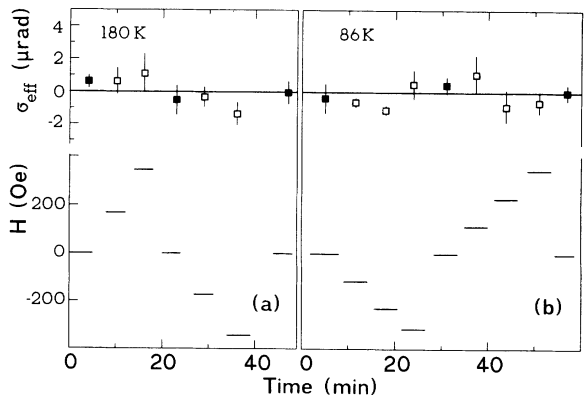

FIG. 11. Field and time dependence of σ_{eff} at 180 and 86 K. Values in zero field are indicated by full symbols.

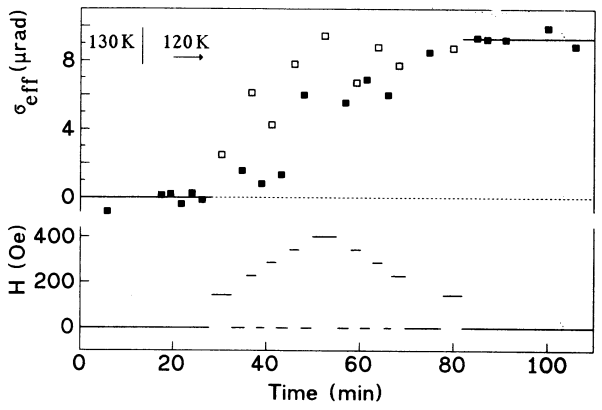

FIG. 12. Field and time dependence of σ_{eff} at 120 K (one value at 130 K). Values in zero field are indicated by full squares.

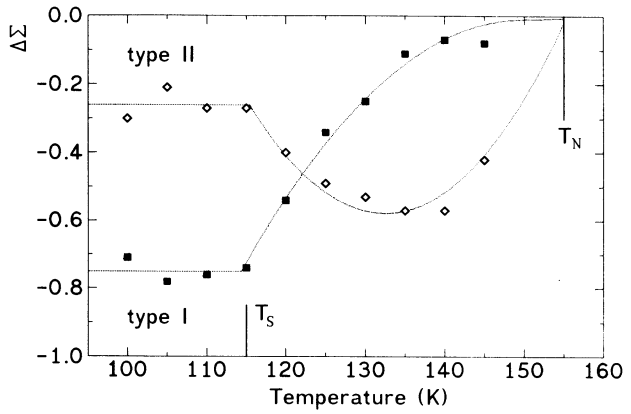

FIG. 13. Relative changes $\Delta\Sigma$ in the spatial scattering of σ_{eff} showing the impact of the magnetic field as explained in the text. Lines are a guide to the eye.

feature of simple anelastic processes but needs viscoelasticity.[39] We also note that the relaxation times present in Fig. 12 are larger than those measured by internal friction. Thus, the coincidence of temperatures for the appearance of field-induced and anelastic relaxation is striking but in detail the mechanisms are different.

Figure 12 shows that the magneto-optical response is enhanced by slow relaxation processes. To avoid a quenching of this enhancement H is used as an annealing field as described in the following. We start at a reference temperature which lies between 170 and 190 K and cool the sample under a static magnetic field of 400 Oe. At 86 K, just above T_c, the field is switched off and the sample is warmed up to the starting temperature in zero field. Again, the field is applied but with a sign opposite to that in the first run and the temperature cycle is repeated. This is the standard procedure for all low-field measurements described below.

To clarify the general features of the impact of H on the material, σ_{eff} is considered for different spots on the sample. The spots are the same as in Fig. 8. The selected temperatures are the same as shown in Figs. 9 and 10. At each temperature for both field cycles and for the zero-field results shown in Figs. 9 and 10, the spatial scattering of σ_{eff} is determined by calculating the standard deviation for the two types of domains. We will denote this by $\Sigma_{\sigma_{eff}}$. Figure 13 shows the relative changes

$$\Delta\Sigma=[\Sigma_{\sigma_{eff}^{MF}}-\Sigma_{\sigma_{eff}^{0}}]/\Sigma_{\sigma_{eff}^{0}}$$

for temperatures below T_N. At 170 K this value is zero. Results are the same for positive and negative annealing fields. The strong negative values for $\Delta\Sigma$ demonstrate that the magnetic field reduces the inhomogeneity of the sample. This can happen as a consequence of the switching of antiferromagnetic domains in order to reduce the deformation energy of grains as discussed in Sec. II B. Both the reduction of inhomogeneity and the remanent impact of the magnetic field are difficult to explain without any magnetic ordering of the material.

C. Violation of T symmetry in low fields

We have performed four different runs in annealing fields of 400 Oe. In run 1, the sign of H while cooling was negative in the first temperature cycle and positive in the second. Before the run is started a position of the sample is selected which shows a minimum for the gradient of spontaneous σ_{eff}^{0} to improve stability. In Fig. 14 the results for the two cycles are presented with shifted temperature scales. We address the differences of values by

$$\Delta\sigma_{odd}=[\sigma^{+}-\sigma^{-}]/2\ ,$$

where superscripts indicate the sign of the annealing field. We have to distinguish between $\Delta\sigma_{odd}^{MF}$ observed on cooling under the action of the field, and $\Delta\sigma_{odd}^{ZF}$, obtained on warming in zero field. At 86 K both quantities show the same value. On warming $\Delta\sigma_{odd}^{ZF}=5.2$ μrad is stable up to

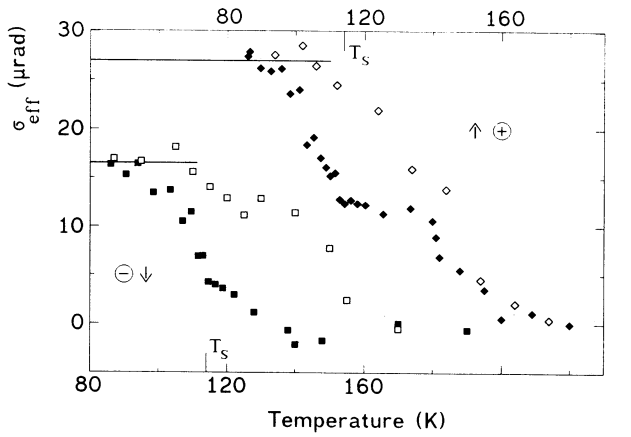

FIG. 14. σ_{eff} during temperature cycles in annealing fields of 400 Oe. The field was applied during cooling only (full symbols). + and − denote the signs of fields. Empty symbols represent data taken on warming in zero field. Note the shifted temperature scales. Solid lines represent the constant effect at low temperatures. Broken lines are a guide to the eye.

about 130 K. This is more clearly demonstrated in Fig. 15. Notice that there is no way to explain the remanence of $\Delta\sigma_{odd}^{ZF}$ without assuming that T symmetry is violated in $YBa_2Cu_3O_{7-x}$. We have checked its stability over a period of four hours. A comparison of the results in Fig. 15 with Eq. (8) reveals that $\Delta\sigma_{odd}^{MF}$ cannot be simple MCD. This subject is discussed below.

Figure 14 gives the impression that σ_{eff} also contains effects which are even in H. To work them out we use the zero-field data σ_{eff}^0 from curve β in Fig. 7. They were measured directly after the temperature cycles in annealing fields had been performed. The magneto-optical response even in H is defined by

$$\Delta\sigma_{even}=[\sigma^+ + \sigma^-]/2-\sigma_{eff}^0 .$$

Results are included in Fig. 15. In calculating $\Delta\sigma_{even}$ and $\Delta\sigma_{odd}$ from the raw data σ_{eff} has been interpolated between two temperatures, if necessary. In Fig. 15 T_S is marked mainly by $\Delta\sigma_{even}^{MF}$, but both quantities appear at T_N. The results for $\Delta\sigma_{even}^{MF}$ can be used to verify that not only the zero-field values of $\Delta\sigma_{odd}$ but also those observed on cooling in the field are a signature of broken T symmetry. We assume for a moment that $\Delta\sigma_{odd}^{MF}$ at 140 K is MCD enhanced by a big magnetostrictive effect. This is a strain induced by H^2. Then one can see from Eq. (4b) that the ratio $S(H^2)/S^0$ is equal to $\Delta\sigma_{even}^{MF}/\sigma_{eff}^0$ which is about 1 at 140 K. S^0 is a spontaneous strain. The term $f'HS^0$ in Eq. (4a) is limited by the uncertainty of the MCD value [Eq. (8)] to less than 0.2×10^{-9} μrad/Oe. This results in an upper limit for a magnetostrictive-enhanced MCD of 0.08 μrad that is a factor of 50 smaller than the observed effect, which therefore cannot be MCD.

The following experiments are performed to confirm the positive results for broken T symmetry. First, run 1 is repeated, but now the sign of H while cooling is positive in the first temperature cycle and negative in the second. Within the experimental accuracy the behavior of $\Delta\sigma_{odd}^{MF}$ and $\Delta\sigma_{odd}^{ZF}$ is the same as shown in Fig. 15. Thus, the appearance of $\Delta\sigma_{odd}$ is not accidental. In run 3 we made the measurements on eight different spots already mentioned. Average results for the two types of domains are given in Fig. 16. The error bars are a measure of the scatter of the spots. Obviously, the significant features of Fig. 15 are reproduced. In detail the data below 135 K show a linear dependence of spontaneous σ_{eff}^0. The slope is $\partial\sigma_{odd}/\partial\sigma_{eff}^0=0.1$. Based on our phenomenological model outlined in Sec. II this dependence is easily understood because $\Delta\sigma_{odd}$ as well as σ_{eff}^0 depends on strains. As can be verified with the help of Figs. 9 and 10, this dependence on strains is responsible for the slight difference in the magnitude of $\Delta\sigma_{odd}$ for the two types of domains. In a final run, measurements are performed on sample B. Just above T_c we observe $\Delta\sigma_{odd}=7$ μrad, which is compatible with the results in sample A. The reproducibility of sign and magnitude of $\Delta\sigma_{odd}$ demonstrates that our idea for a homogenization of the optical response by an external field is reasonable.

With respect to our remarks in Sec. II D, $\Delta\sigma_{odd}$ has to be identified with σ_{NR}, and σ_R as well as σ_M should depend on $|H|$. The latter effect is contained in $\Delta\sigma_{even}^{MF}$. Thus, its existence confirms the consistency of the experimental results with our model. $\Delta\sigma_{even}^{MF}$ obtained in run 1 is already shown in Fig. 15. Figure 17 presents the average results for the two types of domains as observed in the measurements on eight different spots. Most interesting is the big effect for type-II domains at low temperatures. It suggests that the signature of broken T symmetry can be even more pronounced than is shown by $\Delta\sigma_{odd}$. The variation of sign with temperature indicates that $\Delta\sigma_{even}^{MF}$ contains different contributions of opposite sign. This is consistent with the possible occurrence of two different optical quantities. Analyzing the results in detail, $\Delta\sigma_{even}^{MF}$ of all spots exhibits a strong linear dependence on spontaneous σ_{eff}^0. The slope is -1.1 for temperatures below 135 K. The consistency of this result with our model is most easily recognized by a comparison of Eq. (4b) with Eq. (4c). In both equations the same strains are involved. Notice that Eq. (4c) can be expanded to higher order by the same nonlinear strain terms which have been included in Eq. (4b).

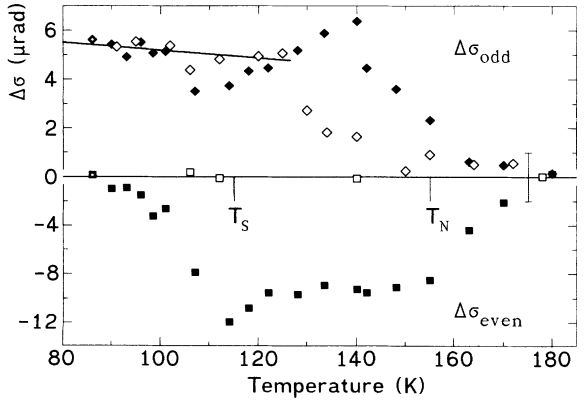

FIG. 15. $\Delta\sigma_{odd}$ ($\Diamond$) and $\Delta\sigma_{even}$ ($\Box$) during temperature cycles in annealing fields of 400 Oe. The field was applied during cooling only (full symbols). Empty symbols represent data taken on warming in zero field. The solid line shows the remanent $\Delta\sigma_{odd}$.

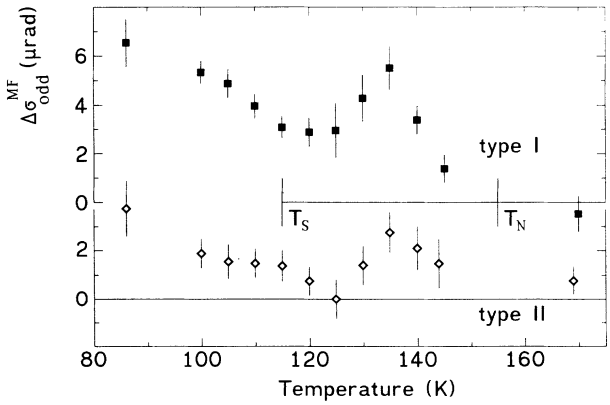

FIG. 16. Average values of $\Delta\sigma_{odd}^{MF}$ for the two types of domains. The error bars correspond to the variation of individual spots.

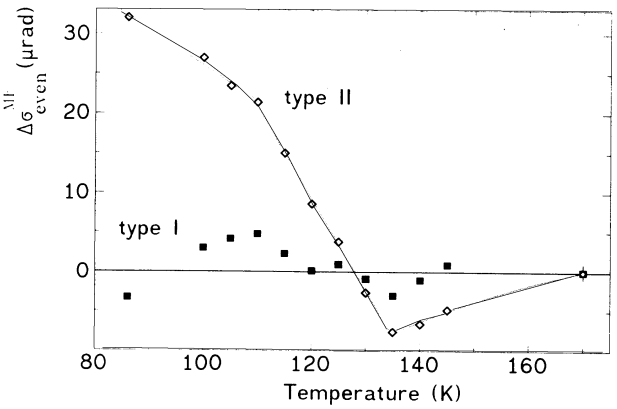

FIG. 17. Average values of $\Delta\sigma_{\text{even}}^{\text{MF}}$ for the two types of domains. The line is a guide to the eye.

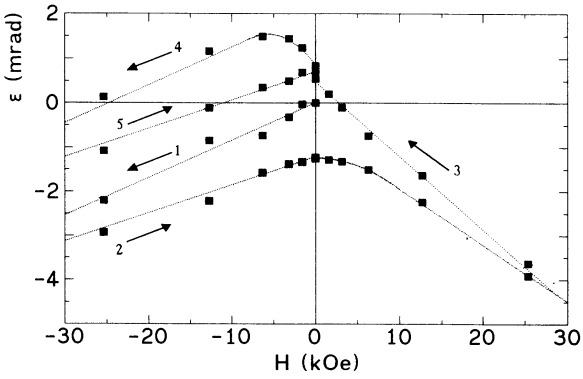

FIG. 18. ϵ during field cycles at 148 K up to fields of 50 kOe. The data for 50 kOe are not shown here, but are included in Fig. 19. Arrows and numbers indicate the way data were taken.

In summarizing the results of our low-field measurements, we point out that they demonstrate the violation of T symmetry and are consistent with several important features of our phenomenological model.

D. Violation of T symmetry in high fields

A dependence on $|H|$ can be distinguished from an H^2 dependence by measurements in high fields. Figure 17 suggests that different contributions are involved in $\Delta\sigma_{\text{even}}^{\text{MF}}$ and that the field dependence can be rather complex for different temperatures. All the measurements produce the same sign for $\Delta\sigma_{\text{even}}^{\text{MF}}$ only between 130 K and T_N. Furthermore, one may expect that the influence of relaxation processes decreases with increasing temperature. We conclude that the intrinsic dependence on H will develop most clearly just below T_N.

The induced ellipticity ϵ is observed in several subsequent field cycles at 148 K. The results for fields up to 30 kOe are shown in Fig. 18. In Fig. 19 the same values and data for 50 kOe are used for a double-logarithmic plot. The slope of the solid lines in Fig. 19 is 1. All values taken on decreasing field strengths obey this dependence. Thus, ϵ is intrinsically proportional to $|H|$. This and the spontaneous ellipticity ϵ^0 with a sign correlated to the sign of H (Fig. 18) prove a violation of T symmetry.

Figure 18 and the inset of Fig. 19 demonstrate an H^2 dependence for increasing field strengths but only for small fields. This behavior is consistent with Eqs. (4c) and (5b) because in this field range the signs of γ' and β^* are switched, which results in an additional H dependence of these material parameters. The difference in the magnitude of the slopes for positive and negative fields and the curvature in cycle 4 of Fig. 18 suggest that the switching process is not reversible in all grains. However, the difference is not clearly outside the limit of the systematic error estimated in Eq. (17) and therefore is not significant.

The remaining ellipticity should be equal to σ_{NR}. Assuming that its magnitude depends on the largest field applied to an experiment, σ_{NR} in Fig. 18 corresponds to a value of 6.9 ± 1.5 μrad for a maximum field of 400 Oe. In low-field measurements we observed the same sign and just above T_c the same magnitude. A similar agreement is not observed for the variation of ϵ in Fig. 19 and $\Delta\sigma_{\text{even}}$ in low-field experiments. σ_R is probably superposed by σ_M in low-field and by σ_{LA} in high-field experiments.

V. CONCLUSION

The strongest proof presented for a violation of T symmetry in $YBa_2Cu_3O_{7-x}$ is the appearance of a persistent optical quantity as a consequence of an applied magnetic field. The reproducibility of this effect in different experiments suggests that our method points a way towards a quantitative characterization of the underlying antiferromagnetic state. The second proof presented is the dependence of the optical response on $|H|$ in the high-field experiments. Figure 18 can be considered to be a typical hysteresis curve of a piezomagnetic antiferromagnet which is permanently stressed during field treatment.

The measured numbers for spontaneous σ_{NR} simply demonstrate that the material is able to exhibit a spontaneous effect between 1 mrad and zero. Therefore, we

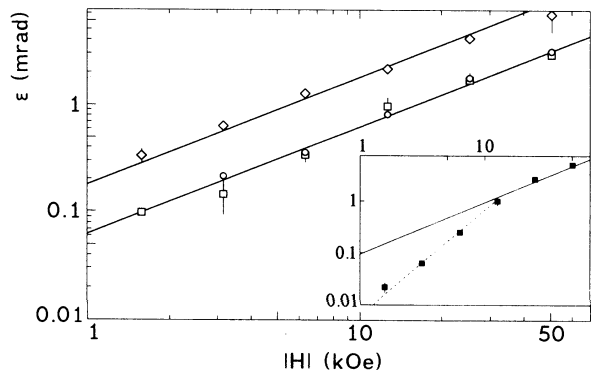

FIG. 19. Double-logarithmic plot of the data of Fig. 18 after subtraction of the zero-field value. Open symbols with decreasing fields, full symbols (inset) with increasing fields. □, ○, ◇ correspond to cycles 2,5,3 in Fig. 18. Solid lines visualize a linear dependence of ϵ on $|H|$ and the broken line (inset) shows an H^2 dependence.

are not able to find a discrepancy between our results and the negative and positive results reported previously.[3-5,10-14] In our phenomenological model an optical response depends on the existence of strains. This predicts an ambivalent behavior of a single crystal. If the sample is an ideal single crystal the optical response should be zero. If there is a residual crystallographic domain hidden in the sample it can react homogeneously on the internal stress. As a consequence the optical response should be bigger than in films. This probably happened in the experiment of Weber *et al.*[4]

In spite of all hints that it may be possible to reconcile conflicting results the observation of differences over several orders of magnitude remains surprising. It can be understood most easily on the basis of a highly nonlinear medium. Nonlinear photoelasticity can be concluded from some of our results. Nonlinear elasticity seems to be a matter of fact in $YBa_2Cu_3O_{7-x}$. We like to note that it can explain the negative result Lyons *et al.*[12] observed in films on $LaAlO_3$. In contrast to MgO this substrate exhibits a smaller lattice constant than $YBa_2Cu_3O_{7-x}$. Then, due to nonlinear elasticity stresses are more effectively transferred from the interface to the free face of a grain. As a consequence the gradients of strains which produce nonreciprocal circular dichroism [Eq. (5a)] are smaller than for a MgO substrate or even completely absent.

ACKNOWLEDGMENTS

We would like to thank M. Lenkens and G. Linker for the $YBa_2Cu_3O_{7-x}$ samples and V. V. Pavlov for the EuS film. This work was supported by the Deutsche Forschungsgemeinschaft.

[1]R. B. Laughlin, Science **242**, 525 (1988).
[2]X. G. Wen and A. Zee, Phys. Rev. Lett. **62**, 2873 (1989).
[3]K. B. Lyons *et al.*, Phys. Rev. Lett. **64**, 2949 (1990).
[4]H. J. Weber *et al.*., Solid State Commun. **76**, 511 (1990).
[5]S. Spielman *et al.*, Phys. Rev. Lett. **65**, 123 (1990).
[6]A. G. Rojo and G. S. Canright, Phys. Rev. Lett. **66**, 949 (1991); A. G. Rojo and A. J. Leggett, *ibid.* **67**, 3614 (1991).
[7]I. E. Dzyaloshinskii, Phys. Lett. A **155**, 62 (1991).
[8]G. S. Canright and A. G. Rojo, Phys. Rev. Lett. **68**, 1601 (1992).
[9]A. L. Shelankov, Phys. Rev. Lett. **69**, 3132 (1992); G. S. Canright and A. G. Rojo, *ibid.* **69**, 1439 (1992).
[10]S. Spielman *et al.*, Phys. Rev. B **45**, 3149 (1992).
[11]S. Spielman *et al.*, Phys. Rev. Lett. **68**, 3479 (1992).
[12]K. B. Lyons *et al.*, Phys. Rev. B **47**, 8195 (1993).
[13]T. W. Lawrence, A. Szöke, and R. B. Laughlin, Phys. Rev. Lett. **69**, 1439 (1992).
[14]H. J. Weber, Int. J. Mod. Phys. B **5**, 1539 (1991).
[15]A. Burau *et al.*, Physica C **216**, 284 (1993).
[16]See, for example, the review articles by J. Dominec, Supercond. Sci. Technol. **6**, 153 (1993); G. Cannelli *et al.*, *ibid.* **5**, 247 (1992).
[17]For example, R. R. Birss, *Symmetry and Magnetism* (North-Holland, Amsterdam, 1966).
[18]For example, L. D. Landau and E. M. Lifschitz, *Elektrodynamik der Kontinua* (Akademie-Verlag, Berlin, 1985).
[19]C. Gerber *et al.*, Nature **350**, 279 (1991).
[20]V. Mueller *et al.*, Solid State Commun. **72**, 997 (1989).
[21]V. P. Martovitsky and V. V. Rodin, Physica C **182**, 269 (1991).
[22]C. Fanggao *et al.*, Phys. Rev. B **43**, 5526 (1991); M. Cankurtaran *et al.*, *ibid.* **46**, 1157 (1992).
[23]H. M. Ledbetter and S. A. Kim, Phys. Rev. B **38**, 11 857 (1988).
[24]G. Cannelli *et al.*, Europhys. Lett. **6**, 271 (1988).
[25]V. A. Melik-Shakhnazarov *et al.*, Pis'ma Zh. Eksp. Teor. Fiz. **50**, 72 (1989) [JETP Lett. **50**, 81 (1989)].
[26]L. N. Pal-Val *et al.*, Solid State Commun. **81**, 761 (1992).
[27]M. Cankurtaran and G. A. Saunder, Supercond. Sci. Technol. **5**, 529 (1992).
[28]B. B. Krichevtsov *et al.*, Pis'ma Zh. Eksp. Teor. Fiz. **54**, 75 (1991) [JETP Lett. **54**, 84 (1991)].
[29]H. J. Weber, Acta Crystallogr. A **35**, 225 (1979).
[30]V. V. Eremenko and N. F. Kharchenko, Phys. Rep. **155**, 379 (1987).
[31]M. K. Kelly *et al.*, Phys. Rev. B **38**, 870 (1989).
[32]D. C. Johnston, J. Magn. Magn. Mater. **100**, 218 (1991).
[33]A. A. Milner *et al.*, Physica C **209**, 225 (1993).
[34]H. Becker *et al.*, Rev. Sci. Instrum. **62**, 1196 (1991).
[35]J. Ferre *et al.*, Solid State Commun. **11**, 1173 (1972).
[36]S. Haussühl and W. Effgen, Z. Kristallogr. **183**, 153 (1988).
[37]H. Izumi *et al.*, Physica C **199**, 171 (1992); J. C. Fabre and A. C. Boccara, Opt. Commun. **93**, 303 (1992).
[38]C. Meingast *et al.*, Phys. Rev. Lett. **67**, 1634 (1991).
[39]For example, A. S. Nowick and B. S. Berry, *Anelastic Relaxation in Crystalline Solids* (Academic, New York, 1972).